Supplemental Material Table of Contents

Supplemental Material

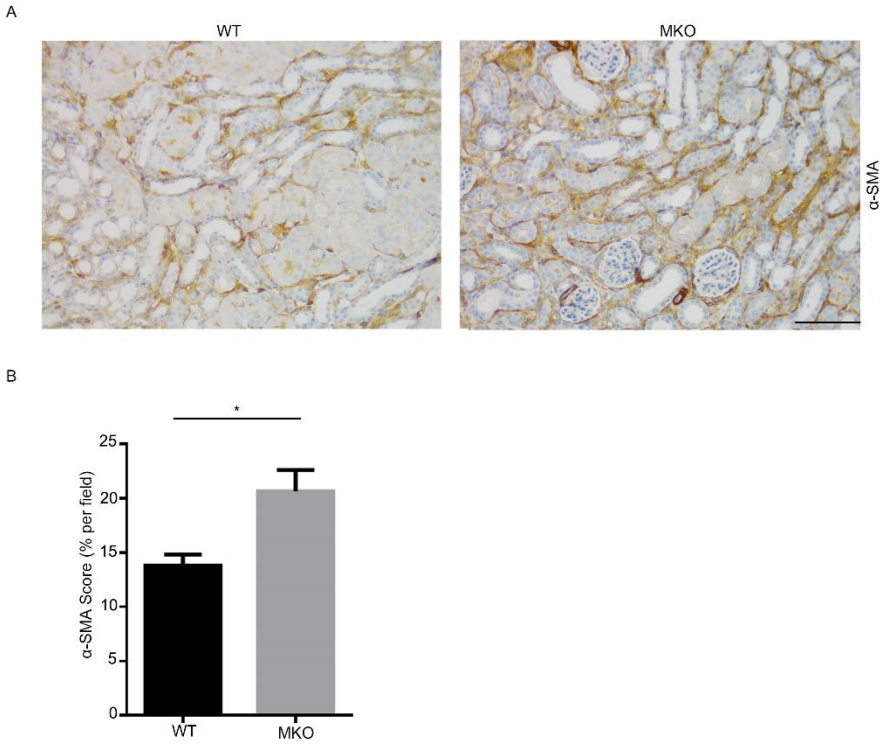

Supplemental Figure 1. Enhanced myofibroblast accumulation in obstructed MKO kidneys. (A) Representative sections from obstructed WT and MKO kidneys stained with α-SMA for myofibroblasts at day 14 UUO. Scale bar = 100 μm (B) Blinded morphometric quantification of α-SMA staining (n=6).

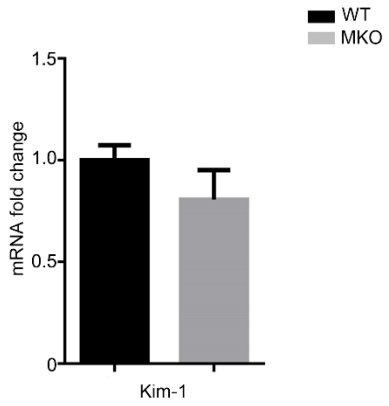

Supplemental Figure 2. mRNA levels of Kim-1 in obstructed WT and MKO kidneys (n≥7).

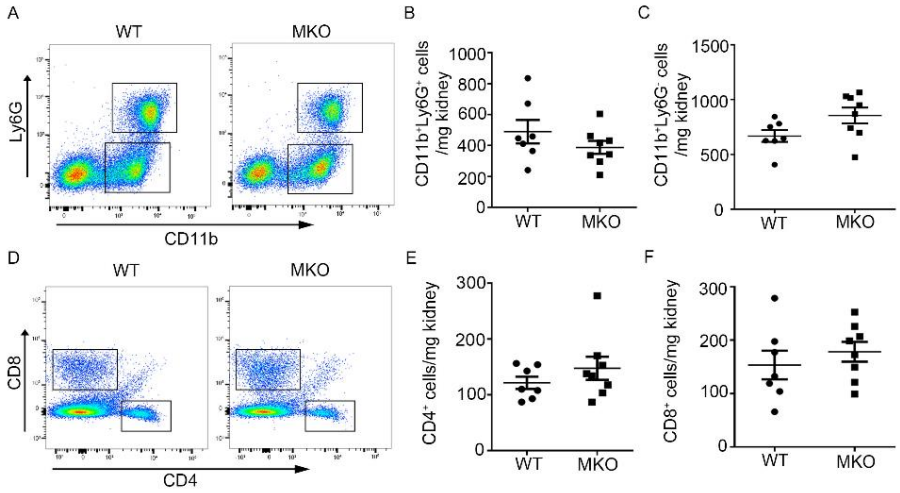

Supplemental Figure 3. Immune cell infiltration into WT and MKO kidneys following UUO. (A, E) Representative flow plots of CD11b versus Ly6G staining (A) and CD4 versus CD8 staining (E) from obstructed kidneys of WT and MKO mice after UUO at 2 weeks. (B, C, F, and G) The number of neutrophils (B), monocytes (C), $CD4^+$ (F) and $CD8^+$ (G) T cells in obstructed WT and MKO kidneys (n=7-8).

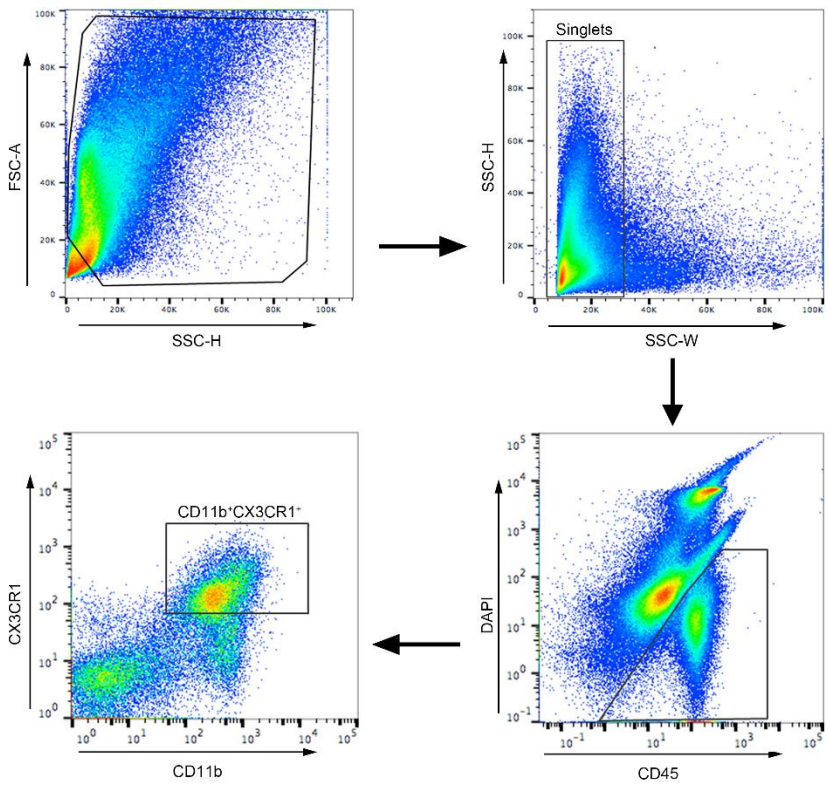

Supplemental Figure 4. The gating strategy for sorting viable CD11b^{+}CX3CR1^{+} myeloid cells from WT and RKO kidneys.